http://ansinet.com/itj

ITJ

ISSN 1812-5638

INFORMATION TECHNOLOGY JOURNAL

ANSInet
Asian Network for Scientific Information
308 Lasani Town, Sargodha Road, Faisalabad - Pakistan

Information Technology Journal 13 (15): 2395-2403, 2014
ISSN 1812-5638 / DOI: 10.3923/itj.2014.2395.2403

Experimental Research on the $LiNi_xCo_yMn_zO_2$ Lithium-ion Battery Characteristics for Model Modification of SOC Estimation

[1]Bizhong Xia, [1]Sa Wang, [1]Yong Tian, [2]Wei Sun, [2]Zhihui Xu and [2]Weiwei Zheng
[1]Graduate School at Shenzhen, Tsinghua University, Shenzhen, 518055, China
[2]Sunwoda Electronic Co. Ltd., Shenzhen, 518108, China

Abstract: The Kalman Filter (KF) known as an optimum adaptive algorithm based on recursive estimation, has been widely used to estimate the State Of Charge (SOC) of the lithium-ion batteries. To improve the performance of SOC estimation, the parameters of battery model in the KF method should be chosen correctly. Nevertheless, the battery parameters, such as the OCV-SOC, capacity and resistance are significantly depended on the battery SOC, temperature, current and ageing. In this study, these dependencies and their variation over the temperature, current and ageing are investigated on a Samsung ICR18650-22P-typed lithium-ion battery with $LiNi_xCo_yMn_zO_2$ cathode which offers guidance to model modification of SOC estimation. The experimental results show that the OCV-SOC relationship are strong consistent under the conditions of 0~60°C but it varies when the temperature remains below zero degrees Celsius. The capacity varies considerably with the temperature and cycles and slightly with the current of below 3C. The Ohmic resistance varies slightly with charge current but considerably with discharge current and SOC. Based on the experimental results, some suggestion for model modification of SOC estimation is put forward.

Key words: Lithium-ion battery, state of charge, battery characteristics, model modification

INTRODUCTION

With the soaring energy shortage and environment deterioration, Electric Vehicles (EVs) have been rapidly developed in recent years (Gong *et al*., 2013; Tian *et al*., 2013). As the main part of energy carrier and power source, power battery affects both the economic and driving performance of the EVs. Lithium-ion battery is widely used for its high performance in energy density, power density, life cycle and so on (Cho *et al*., 2012). The performance of lithium-ion battery is seriously affected by the cathode material, such as $LiFePO_4$, $LiCoO_2$, $LiMn_2O_4$ and $LiNi_xCo_yMn_zO_2$ (x+y+z = 1). Compared with other material, $LiNi_xCo_yMn_zO_2$ has the advantages of high energy density, excellent consistency, mild thermal stability, low cost and low toxicity (Guo *et al*., 2009; Pan *et al*., 2013). Due to these characteristics, $LiNi_xCo_yMn_zO_2$ lithium-ion battery has a promising widespread application on EVs. In order to improve the safety and capability of the battery, a Battery Management System (BMS) is required. As one of the most important functions, SOC estimation should be included to prevent the battery from being over-charged and over-discharged and to manage the energy flows of the EVs. Several methods, such as Ampere-hour (Ah) counting (Lu *et al*., 2013), Open-Circuit Voltage (OCV) (Lee *et al*., 2008), Artificial Neural Network (ANN) (Charkhgard and Farrokhi, 2010; Capizzi *et al*., 2011; Kang *et al*., 2014) and Kalman Filter (KF) (Lee *et al*., 2007; He *et al*., 2011; Dai *et al*., 2012; He *et al*., 2013; Xiong *et al*., 2014; Sepasi *et al*., 2014; Xing *et al*., 2014) have been proposed to estimate the battery SOC. The KF algorithm has been widely employed for online SOC estimation due to its high performance under dynamic driving conditions. KF is a model-based method (Song *et al*., 2012; Ma *et al*., 2013) and as a result, the model parameters should be chosen correctly to improve the estimation performance. However, the parameters of the battery model, such as the OCV-SOC, capacity and resistance are significantly depended on the battery SOC, temperature, current and ageing.

There have been some efforts to resolve these problems. The various OCV-SOC relationships caused by the difference in capacity among cells were discussed (Lee *et al*., 2008). The difference in internal resistance among cells was dealt with by choosing the internal resistance as a state-variable (He *et al*., 2013). The different equilibrium potentials during charge and discharge process at the same SOC were considered and the OCV was defined as the average value of the equilibrium potentials of charge and discharge process to simplify the model (He *et al*., 2011). In this study, it can

Corresponding Author: Yong Tian, Graduate School at Shenzhen, Tsinghua University, Shenzhen, 518055, China

be seen that only a single parameter variation was taken into consideration, besides, the parameter variations with temperature and ageing are often neglected.

In order to obtain more accurate SOC estimation by modification of the battery model, in this study, aforementioned dependencies and their variation over the battery SOC, temperature, current and ageing are investigated on an ICR18650-22P-typed lithium-ion battery with $LiNi_xCo_yMn_zO_2$ cathode produced by Samsung. Several experiments are implemented to obtain the battery characteristics. Based on the experimental results, several correction factors and suggestion for modification of the battery model are put forward.

BATTERY MODEL AND SOC ESTIMATION

A battery model is crucial to SOC estimation using the KF algorithm. Various models have been proposed to simulate the electrochemical characteristics of a lithium-ion battery. The equivalent circuit model, consisting of resistor, capacitor and inductor performs well in describing the dynamic characteristics and as a result, it is usually used in battery SOC estimation (Hu *et al*., 2012; Li *et al*., 2013). A simple equivalent circuit model is shown in Fig. 1, where, OCV, I, R_0 and V_b represent the open-circuit voltage, current, Ohmic resistance and terminal voltage of the battery, respectively and OCV varies with SOC.

Based on Fig. 1, the space-state functions of the battery model can be derived as shown in Eq. 1 and 2:

$$SOC(k) = SOC(k-1) - \frac{I(k-1)\times\Delta t}{Q_N} \quad (1)$$

$$V_b(k) = OCV[SOC(k-1)] - R_0 \times I(k-1) \quad (2)$$

where, Q_N is the normal capacity of the battery.

Usually, Q_N and R_0 are selected as constant which results in large model error due to the fact that they are significantly depended on the battery SOC, temperature, current and ageing. These dependencies will be studied in the following part of this study.

EXPERIMENTAL RESULTS AND DISCUSSION

Experimental configurations: The $LiNi_xCo_yMn_zO_2$ lithium-ion batteries used in the experiments are Samsung ICR18650-22P type with a normal capacity of 2200 mAh (0.2°C discharge at temperature of 25±5°C), a minimum capacity of 2150 mAh (0.2°C discharge at temperature of 25±5°C), a normal voltage of 3.6 V, a charging voltage of 4.2 V and a discharge cut-off voltage of 2.75 V. The experimental equipment is consisted of a power supply, an electric load, a constant temperature and humidity chamber, an Electrochemical Impedance Spectroscopy (EIS) instrument, a control board and a Personal Computer (PC), as shown in Fig. 2. In the experiments, the temperature was set in the range of -20, +60°C which is the storage temperature suggested by the battery specification.

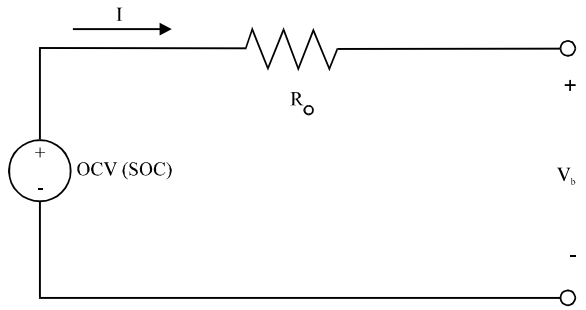

Fig. 1: A simple battery model

Voltage SOC characteristics

Terminal voltage variation with different capacity test: At the temperature of 25±2°C, the battery was charged with a constant current of 100 mA until the charging voltage of 4.20 V and the terminal voltage was recorded simultaneously. Then the battery was rest for 2 h to reach the steady state. Afterwards, the battery was discharged with the same constant current of 100 mA until the cut-off voltage of 2.75 V. The measured terminal voltage variations with the charge and discharge capacity (Q) are shown in Fig. 3.

It can be seen that the terminal voltage variation at the charge process is similar to that at the discharge process. However, they have different values at the same SOC or rather the terminal voltage at the charge process is higher than at the discharge process. This difference in terminal voltage is the reason that the different OCV-SOC relationship during the charge and discharge process. And this difference should be taken into account when a battery model is built. For example, the OCV is redefined as the average value of the charging and discharging equilibrium potentials to improve the SOC estimation accuracy and simplify the battery model, meanwhile, the OCV measured as a function of the SOC was obtained by the quadratic curve fitting method (He *et al*., 2011).

OCV-SOC variation with temperature test: At the temperature of 25±2°C, the battery was firstly charged to the charge voltage of 4.2 V and was rest for 3 h to reach the steady state. Afterwards, it was discharged with a

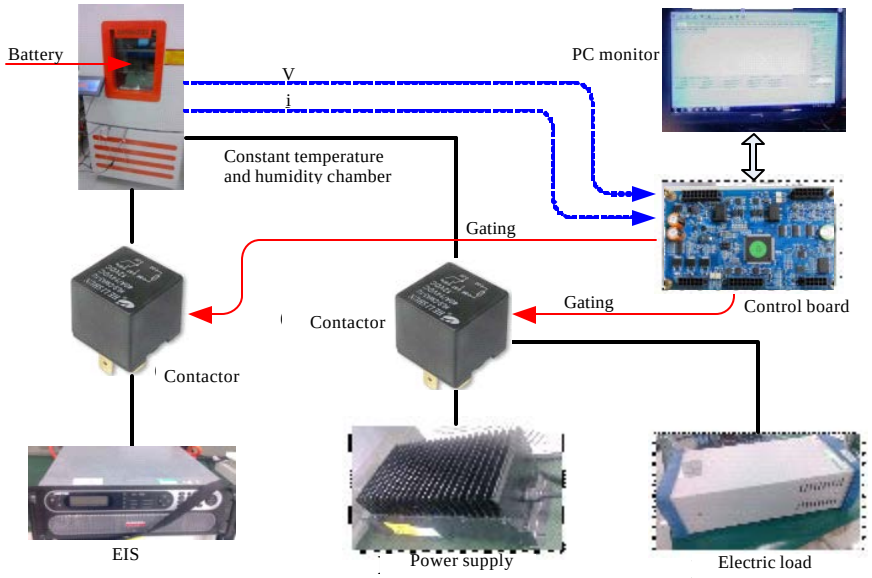

Fig. 2: Experimental equipment

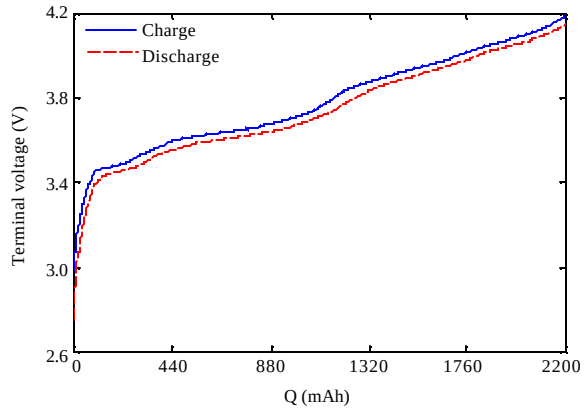

Fig. 3: Realtionship between terminal voltage and capacity

constant current of 0.3C A from the fully charged state to 98% of the actual capacity which will be introduced in the following part of this study. Then, it was left in the open-circuit condition and the terminal voltage was measured after 3 h. The measured terminal voltage is chosen to be the OCV as the change of the terminal voltage is negligible and the battery is assumed to already reach the steady state. Then, the battery was continuously discharged by a further 95, 90, 80, 70, 60, 50, 40, 30, 20, 10, 8, 5, 3, 2, 1 and 0% of the actual capacity with the same current and the OCV was measured after 3 h, respectively.

These steps were repeated under the same charge temperature of 25±2°C and different discharge temperature

Table 1: OCV (V) at different SOC and different temperature

	Temperature (°C)					
SOC (%)	-20°	0°	10°	25°	40°	60°
100	4.167	4.166	4.168	4.177	4.171	4.166
98	4.134	4.135	4.137	4.148	4.140	4.134
95	4.098	4.103	4.104	4.117	4.105	4.100
90	4.056	4.067	4.067	4.080	4.067	4.061
80	3.977	4.004	4.004	4.012	4.001	3.994
70	3.901	3.931	3.931	3.941	3.928	3.925
60	3.834	3.854	3.866	3.878	3.866	3.862
50	3.736	3.747	3.748	3.764	3.755	3.746
40	3.651	3.663	3.661	3.674	3.666	3.668
30	3.592	3.621	3.620	3.633	3.628	3.630
20	3.538	3.585	3.587	3.595	3.581	3.573
10	3.540	3.498	3.501	3.504	3.497	3.488
8	3.515	3.474	3.474	3.484	3.471	3.468
5	3.504	3.454	3.455	3.468	3.456	3.453
3	3.535	3.443	3.444	3.456	3.445	3.441
1	3.505	3.438	3.429	3.436	3.428	3.416
0	3.492	3.434	3.411	3.407	3.406	3.378

of [-20, 0, 10, 40, 60]°C, respectively. The measured OCV at different SOC and different temperature are shown in Table 1. Furthermore, the corresponding OCV-SOC curves are shown in Fig. 4.

From Fig. 4, it can be found that at the different temperature of [0, 10, 25, 40, 60]°C, the OCV-SOC curves have a similar trend. However, the situation becomes obviously different under the temperature of -20°C. Based on these facts, it is suggested that to improve the accuracy of the battery model, different OCV-SOC functions should be used under the condition of high temperature and that of low temperature, respectively.

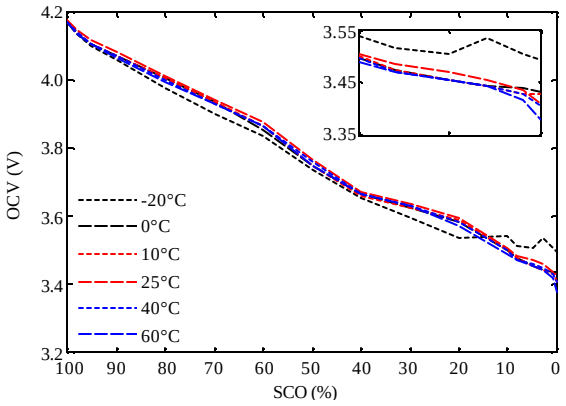

Fig. 4: OCV-SOC curves at different temperature

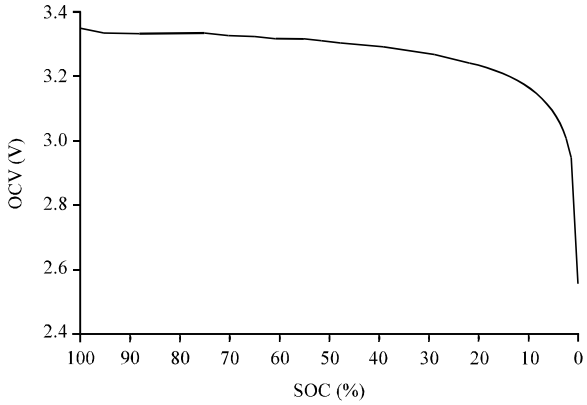

Fig. 5: OCV-SOC curve of a typical $LiFePO_4$ battery

Moreover, it can be seen that there is no voltage platform that exits on the OCV-SOC curve for a $LiFePO_4$ lithium-ion battery, as shown in Fig. 5 (Huria *et al*., 2014; Sepasi *et al*., 2014). As a result, some empirical models used for other kinds of lithium-ion batteries are no longer suitable for $LiNi_xCo_yMn_zO_2$ battery. From Fig. 4, it is clear that a high-order polynomial should be able to describe nonlinear relationship between the OCV and the SOC of a $LiNi_xCo_yMn_zO_2$ battery. However, this will increase the complexity of the stability and computation cost of the SOC estimator. To solve this problem, segmented linear functions (Habiballah *et al*., 2014; Chen *et al*., 2014) have been proposed and each of them can be described as shown in Eq. 3:

$$OCV = f(SOC) = b_0+b_1SOC \quad (3)$$

Capacity characteristics

Discharge capacity variation with temperature test: At the temperature of [-20, -10, 0, 10, 25, 40, 60]°C, the battery was discharged with a constant current of 0.3C A from the fully charged state to the cut-off voltage, respectively and the terminal voltage as well as the discharge capacity calculated by Ah method were recorded simultaneously. The recorded terminal voltage and discharge capacity are shown in Fig. 6.

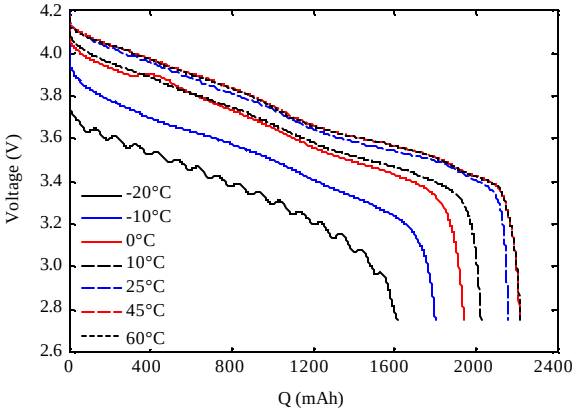

Fig. 6: Voltage-Q curves at different temperature

From Fig. 6, it can be seen that the discharge capacity decreases as the temperature decreases. The decline becomes significant when the temperature decreases to under 0°C. At the temperature of -20°C, the discharge capacity is reduced to about 70% of the normal value. The discharge characteristic at the temperature of 45°C is very close to that at the temperature of 60°C. It is shown that under the condition of high temperature, the potential discharge capacity is larger. However, high temperature is bad for both the life cycle and safety usage of the battery. Therefore, avoiding of working at high temperature is still essential to the battery.

To compensate the model error caused by capacity variation with temperature, a correction factor marked as K_T is introduced which is defined as:

$$K_T = \frac{\text{Capacity at the temperature of Tx °C}}{\text{Capacity at the temperature of 25 °C}}$$

The relationship between K_T and temperature T is shown in Fig. 7, where, the blue-circles are the measured data and the read-line is obtained according to a fitting formula as shown in Eq. 4. It is clear that the introduced formula can describe the battery capacity variation with temperature very well. Thus, such a method can be used to online correct the model error caused by the ambient temperature variation to improve the SOC estimation accuracy.

$$K_T = -5.063\times10^{-5}\times T^2+0.00518T+0.904 \quad (4)$$

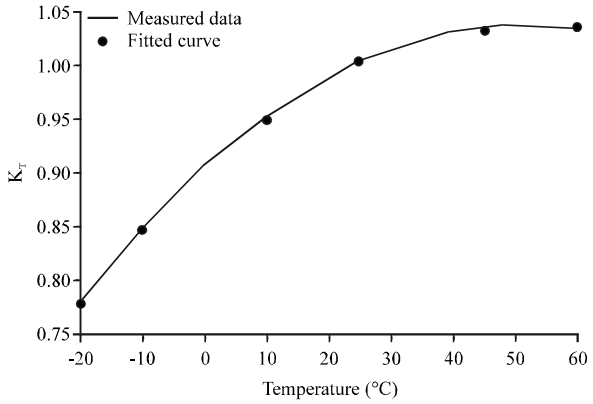

Fig. 7: Relationship between K_T and temperature

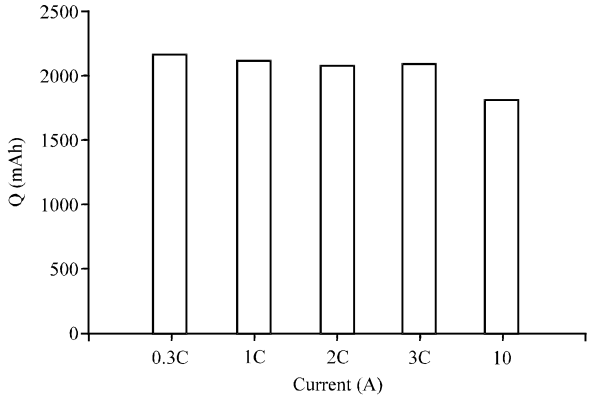

Fig. 8: Capacity under different discharging rate

Capacity variation with discharge rate: At the temperature of 25±2°C, the battery was firstly charged to the charge voltage of 4.2 V and was rest for 10 min. Afterwards, it was discharged with a constant current of 0.3C A until the cut-off voltage and the discharge capacity calculated by Ah method was recorded.

At the same temperature, the foregoing procedure was repeated with different discharge current of [1C, 2C, 3C, 10] A, respectively. The results are shown in Fig. 8. It can be seen that the potential capacity decreases with the increase of the discharge current. An obvious decrease turns up at the max discharge current of 10 A. Hence discharging with a high current is endeavored to avoid in practical application to increase the discharge capacity of a battery.

To compensate the model error caused by capacity variation with discharge rate, a correction factor marked as K_I is introduced which is defined as:

$$K_I = \frac{\text{Capacity under different discharge rate}}{\text{Norminal capacity}}$$

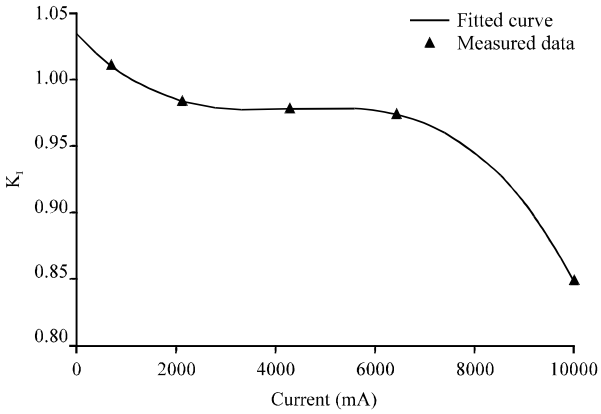

Fig. 9: Relationship between K_I and discharge current

The relationship between K_I and discharge current is shown in Fig. 9, where, the blue-triangles are the measured data and the read-line is obtained according to a fitting formula as shown in Eq. 5. It is clear that this formula can describe the battery capacity variation with operating current very well. Thus, such a method can be used to online correct the model error caused by the operating current variation to improve the SOC estimation accuracy.

$$K_I = -7.571\times10^{-3}\times I^3+9.897\times10^{-9}\times I^2-4.198\times10^{-5}\times I+^21.035 \quad (5)$$

Capacity variation with ageing: At the temperature of 25±2°C, the battery was charged with a constant current of 0.5C A to the voltage of 4.1 V. After rest for 10 min, the battery was discharged with a current of 1C A to the voltage of 3 V and then rest for 10 min. It should be indicated that discharging the battery from 3-4.1 V represents 80% DOD (Depth Of Discharge). After this foregoing cycle repeated for 50 times, the battery was then charged with a constant current of 0.5C A to 4.2 V and rest for 10 min. Then the battery was discharged with a current of 1C A to 2.75 V (100% DOD).

The foregoing procedure was repeated for 900 times to investigate the capacity variation with aging and the results are shown in Fig. 10, where the red-circles and blue-line represent the capacity of 100% DOD and that of 80% DOD, respectively.

From Fig. 10, it can be seen that the capacity loss resists during the charging and discharging process. Nevertheless the distinction of capacity loss is not obvious between that under 100% DOD and that under 80% DOD. After 900 cycles, about 15% of the original capacity has been lost. Thus actual capacity reduction should be considered to improve the accuracy of SOC estimation.

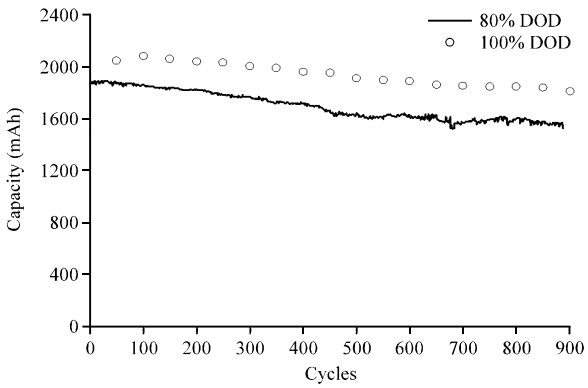

Fig. 10: Capacity variation with ageing

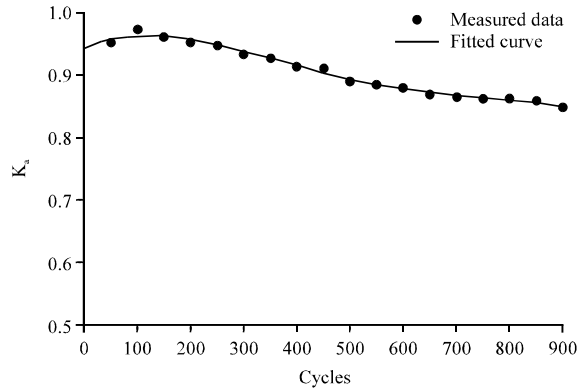

Fig. 11: Relationship between K_a and cycle number

To compensate the model error caused by ageing, a correction factor marked as K_a is introduced which is defined as:

$$K_a = \frac{\text{Capacity at the cylces of a}}{\text{Initial capacity}}$$

The relationship between K_a and the cycles a is shown in Fig. 11, where, the blue-circles represent the measured capacity of 100% DOD and the red-line is obtained according to a fitting formula as shown in Eq. 6. Obviously, the introduced formula can describe the battery capacity variation with aging very well. Thus, such a method can be used to online correct the model error caused by the aging variation to improve the SOC estimation accuracy.

$$K_a = -1.225\times10^{12}\times a^4+2.726\times10^{-9}\times a^3-1.980\times10^{-6}\times a^2+3.610\times10^{-4}\times a+0.942 \quad (6)$$

Ohmic resistance characteristics

Ohmic resistance variation with SOC test: The battery was discharged with a constant current of 0.5C A until the cut-off voltage at the temperature of 25±2°. After a rest of 10 min, it was charged with the same constant current of 0.5C A till the SOC reaches 5% and the Ohmic resistance was measured after a rest of 3 h. Then, the battery was charged to 20, 50, 80 and 100% of the normal capacity, respectively and the corresponding ohmic resistance was measured after a rest of 3 h. At the same temperature, the procedure above was repeated with different charge current of 1C A. The results are shown in Table 2 and Fig. 12.

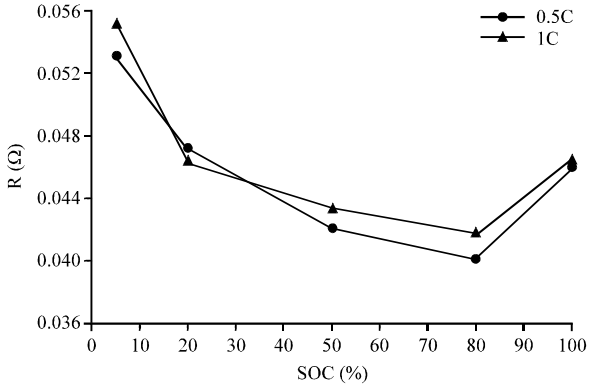

Fig. 12: Charge Ohmic resistance

Table 2: Charge Ohmic resistance Ω at different SOC and different current

	SOC (%)				
Current (C)	5	20	50	80	100
0.5	0.0530	0.0471	0.0420	0.0400	0.0459
1	0.0551	0.0463	0.0433	0.0416	0.0464

From Fig. 12, it can be seen that with the current of 0.5C A, the difference between the highest and the lowest ohmic resistance is 0.013 Ω and the value is 0.0135 Ω under the current of 1C A. The highest difference between the ohmic resistance under 0.5C A and 1C A is 0.0021 Ω. Therefore, a conclusion can be drawn that the charge current has not obviously effect on the ohmic resistance at the same SOC and SOC is the main factor that leads ohmic resistance variation as shown in Eq. 6. Moreover, the Ohmic resistance variation with SOC performs as V-shape and the highest values appear when the battery is fully charged.

At the temperature of 25°C, the battery was charged with a constant current of 0.3C A till the charge voltage of 4.2V and the ohmic resistance was measured after a rest of 3 h. Then it was discharged to the 80, 50 and 20% of the normal capatity, respectively and the ohmic resistance was measured after the same rest time. At the same temperature, the procedure above was repeated with different discharge current of 1C and 2C A, respectively. The results are shown in Table 3 and Fig. 13.

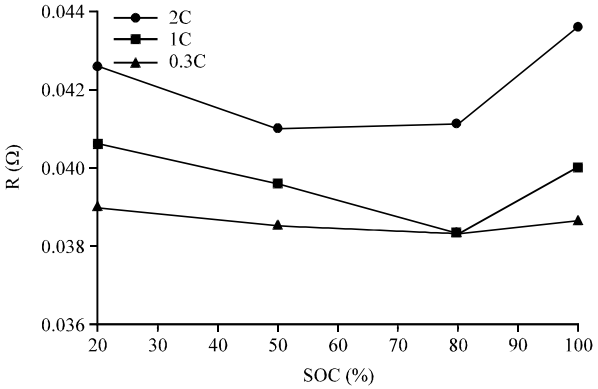

Fig. 13: Discharge ohmic resistance

Table 3: Discharge ohmic resistance (Ω)

	SOC (%)			
Current (C)	20	50	80	100
0.3	0.0390	0.0385	0.0383	0.0387
1	0.0406	0.0396	0.0383	0.0400
2	0.0426	0.0410	0.0411	0.0436

From Fig. 12, it can be found that the ohmic resistance increases as the discharge current increases at the same SOC. Under the condition of different discharge rate, the biggest difference between the ohmic resistances is 0.0049 Ω. And the current rate has more obvious effect on the discharge ohmic resistance than that on the charge ohmic resistance. The variation of ohmic resistance with SOC also performs as V shape and the highest values appear when the battery is fully discharged. The variation is gentle under a low rate.

From Fig. 12 and 13, it is indicated that the ohmic resistance of battery is not a constant but varies with current, SOC, etc. Therefore, large error of SOC estimation is almost resulted by battery model with a constant ohmic resistance. To resolve this problem, ohmic resistance is also selected as a state-variable and estimated in real-time (He *et al*., 2013). Unfortunately, it increases the computation cost obviously. Thus, more efforts have to be made to improve the model accuracy.

SOLUTIONS FOR ACCURATE SOC ESTIMATION

Based on the experimental results of this study, it is suggested that two solutions can be used to improve the accuracy of SOC estimation. The first one is to update the parameters of battery model, e.g., normal capacity, internal resistance, etc., based on its operating conditions, including SOC, temperature, current and ageing. This method is called static correction method in this study. For instance, the SOC updating function in Eq. 1 can be rewritten as in Eq. 7 by using the static correction method. Furthermore, defining the SOC in term of energy balance can be more accurate as the energy loss due to the internal resistance is not ignorable under the condition of high current discharging or charging. And the definition of SOC can be expressed as in Eq. 8 according to Fig. 1, where, E_b is the average equilibrium potential of battery:

$$SOC(k) = SOC(k-1) - \frac{I(k-1)\times\Delta t}{K_T K_I K_a Q_N} \quad (7)$$

$$SOC(k) = SOC(k-1) - \frac{(V_b + R_o \times I(k-1))\times I(k-1)\times\Delta t}{(K_T K_I K_a Q_N)\times E_b} \quad (8)$$

The second one is called as dynamic correction method in this study. It is to employ intelligent algorithms with superior estimation performance, such as Kalman filtering, sliding mode observer and their modified method, etc. Although this method has been widely used in recently years and reported in many literatures. It has some drawbacks such as dependency on model accuracy, high requirement for hardware, high computation cost, etc. Therefore, algorithms with more superior performance are still required to improve the SOC estimation accuracy under the conditions of model error, measurement error and operating condition variation.

CONCLUSION

In order to improve the model accuracy of SOC estimation, this study based on the characteristics of Samsung ICR18650-22P-typed lithium-ion battery with $LiNi_xCo_yMn_{1-x-y}O_2$ cathode that is being applied more and more in electric vehicles for its excellent performance. Several experiments have been implemented to obtain the dependency of OCV-SOC relationship, capacity and ohmic resistance on the battery SOC, temperature, current and ageing. The experimental results can be concluded as follows:

- The terminal voltage variation at the charge process is similar to that at the discharge process. However, they have different values at the same SOC which is the reason that the different OCV-SOC relationship during the charge and discharge process. And this difference should be taken into account when a battery model is built
- At the different temperature of [0, 10, 25, 40 and 60]°C, the battery OCV-SOC relationship has a similar trend and the cut-off voltage decreases as the temperature rises. However, the situation becomes obviously different at the temperature of -20°C. Thus, it is suggested that different OCV-SOC functions should be used under the condition of high temperature and that of low temperature, respectively

- On the OCV-SOC curve of $LiNi_xCo_yMn_zO_2$ battery, there is no voltage platform that exits on the curve for a $LiFePO_4$ battery. Therefore, some empirical model used for other kinds of battery is not suitable for $LiNi_xCo_yMn_zO_2$ battery
- The discharge capacity decreases as the temperature decreases. At the temperature of -20°C, the capacity is even reduced to about 70% of the normal value
- The potential capacity decreases with the increase of discharge current. Hence, it is suggested that a battery should be prevented from discharging with a high current to increase the discharge capacity
- The actual capacity fades with ageing. After 900 cycles of charging and discharging, about 15% of the original capacity has been lost. This fading should be taken into account when estimating the SOC of a long-term used battery
- The ohmic resistance of battery is not a constant but varies with current, SOC, etc. and its variation with SOC performs as V shape. Therefore, large error of SOC estimation is almost resulted by battery model with a constant ohmic resistance

ACKNOWLEDGMENTS

This study is supported by the China Postdoctoral Science Foundation Funded Project (2013M540941) and the Shenzhen Key Laboratory of LED Packaging Funded Project (NZDSY20120619141243215).

REFERENCES

Capizzi, G., F. Bonanno and C. Napoli, 2011. Hybrid neural networks architectures for SOC and voltage prediction of new generation batteries storage. Proceedings of the International Conference on Clean Electrical Power, June 14-16, 2011, Ischia, pp: 341-344.

Charkhgard, M. and M. Farrokhi, 2010. State of charge estimation for lithium-ion batteries using neural networks and EKF. IEEE Trans. Ind. Electron., 57: 4178-4187.

Chen, X., W. Shen, Z. Cao and A. Kapoor, 2014. A novel approach for state of charge estimation based on adaptive switching gain sliding mode observer in electric vehicles. J. Power Sour., 246: 667-678.

Cho, S., H. Jeong, C. Han, S. Jin, J. Lim and J. Oh, 2012. State-of-charge estimation for lithium-ion batteries under various operating conditions using an equivalent circuit model. Comput. Chem. Eng., 41: 1-9.

Dai, H., X. Wei, Z. Sun, J. Wang and W. Gu, 2012. Online cell SOC estimation of li-ion battery packs using a dual time-scale Kalman filtering for EV applications. Applied Energy, 95: 227-237.

Gong, X., T. Lin and B. Su, 2013. Two approaches for coordination of electric vehicle charging and the comparison. J. Applied Sci., 13: 2891-2896.

Guo, R., P. Shi, X. Cheng, Y. Ma and Z. Tan, 2009. Effect of Ag additive on the performance of $LiNi_{1/3}Co_{1/3}Mn_{1/3}O_2$ cathode material for lithium ion battery. J. Power Sour., 189: 2-8.

Habiballah, R.E., F. Baronti and M.Y. Chow, 2014. Online adaptive parameter identification and state-of-charge coestimation for lithium-polymer battery cells. IEEE Trans. Ind. Electron., 61: 2053-2061.

He, H., R. Xiong, X. Zhang, F. Sun and J. Fan, 2011. State-of-Charge estimation of the lithium-ion battery using an adaptive extended Kalman filter based on an improved thevenin model. IEEE Trans. Veh. Technol., 60: 1461-1469.

He, W., N. Williard, C. Chen and M. Pecht, 2013. State of charge estimation for electric vehicle batteries using unscented Kalman filtering. Microelectron. Reliab., 53: 840-847.

Hu, C., B.D. Youn and J. Chung, 2012. A multiscale framework with extended Kalman filter for lithium-ion battery SOC and capacity estimation. Applied Energy, 92: 694-704.

Huria, T., G. Ludovici and G. Lutzemberger, 2014. State of charge estimation of high power lithium iron phosphate cells. J. Power Sour., 249: 92-102.

Kang, L.W., X. Zhao and J. Ma, 2014. A new neural network model for the state-of-charge estimation in the battery degradation process. Applied Energy, 121: 20-27.

Lee, J., O. Nam and B.H. Cho, 2007. Li-ion battery SOC estimation method based on the reduced order extended Kalman filtering. J. Power Sour., 174: 9-15.

Lee, S., J. Kim, J. Lee and B.H. Cho, 2008. State of charge and capacity estimation of lithium-ion battery using a new open-circuit voltage versus state-of-charge. J. Power Sour., 185: 1367-1373.

Li, J., J.K. Barillas, C. Guenther and M. Danzer, 2013. A comparative study of state of charge estimation algorithms for $LiFePO_4$ batteries used in electric vehicles. J. Power Sour., 230: 244-250.

Lu, L., X. Han, J. Li, J. Hua and M. Ouyang, 2013. A review on the key issues for lithium-ion battery management in electric vehicles. J. Power Sour., 226: 272-288.

Ma, L.H., K.L. Wang and H. Li, 2013. Gyrocompass alignment method of sins based on Kalman filtering pretreatment and dynamic gain adjustment on a rocking base. Inform. Technol. J., 12: 777-783.

Pan, C.C., C.E. Banks, W.X. Song, C.W. Wang, Q.Y. Chen and X.B. Ji, 2013. Recent development of $LiNi_xCo_yMn_zO_2$: Impact of micro/nano structures for imparting improvements in lithium batteries. Trans. Nonferrous Metals Soc. China, 23: 108-119.

Sepasi, S., R. Ghorbani and B.Y. Liaw, 2014. Improved extend Kalman filter for state of charge estimation of battery pack. J. Power Sour., 255: 368-376.

Song, H., Y. Fu and X. Liu, 2012. An adaptive UKF algorithm for single observer passive location in non-Gaussian environment. Inform. Technol. J., 11: 1251-1257.

Tian, Y., B. Xia and Y. Sun, 2013. Segmented tracks planning of roadway-powered system for electric vehicles using improved particle swarm optimization. Inf. Technol. J., 12: 1547-1554.

Xing, Y., W. He, M. Pecht and K.L. Tsui, 2014. State of charge estimation of lithium-ion batteries using the open-circuit voltage at various ambient temperatures. Applied Energy, 113: 106-115.

Xiong, R., F. Sun, X. Gong and C. Gao, 2014. A data-driven based adaptive state of charge estimation of lithium-ion polymer battery used in electric vehicles. Applied Energy, 113: 1421-1433.